Polymerizable Complex Synthesis of $RuO_2/BaTi_4O_9$ Photocatalysts at Reduced Temperatures: Factors Affecting the Photocatalytic Activity for Decomposition of Water

Yohichi Yamashita and Kiyohide Yoshida

Riken Corporation, Suehiro 4-14-1, Kumagaya City, Saitama 360-0016, Japan

Masato Kakihana*

Materials and Structures Laboratory, Tokyo Institute of Technology, Nagatsuta 4259, Midori-ku,Yokohama 226-8503, Japan

Satoshi Uchida and Tsugio Sato

Institute for Chemical Reaction Science, Tohoku University, Katahira 2-1-1, Aoba-ku, Sendai 980-0812, Japan

Received June 3, 1998. Revised Manuscript Received October 27, 1998

Phase-pure $BaTi_4O_9$ powders were prepared at temperatures higher than 700 °C by the Pechini-type polymerizable complex (PC) technique, based upon polyesterification between citric acid and ethylene glycol. $BaTi_4O_9$ was subsequently converted to nanocomposite materials by modifying its surface with ultrafine particles of RuO_2, and the nanocomposite was used as photocatalyst for the decomposition of water into H_2 and O_2. The RuO_2/PC-$BaTi_4O_9$ material prepared at 800 °C showed a photocatalytic activity ∼5 times higher than that of a sample prepared by a solid-state reaction at 1100 °C. The activity did not scale simply with the specific surface area of the samples; e.g. the sample having a surface area of 20.4 m^2/g (prepared at 700 °C) showed, unexpectedly, a ∼50% reduction in the activity when compared with that of a sample having a surface area of 7.6 m^2/g (prepared at 800 °C). The anomalous reduction in the activity was interpreted as a consequence of the increased number of lattice defects acting as inactivation centers. The average emission lifetime estimated from an emission decay curve decreased from 4.0 to 2.5 ns with a decrease in the preparation temperature from 900 to 700 °C, suggesting that the number of lattice defects is increased as the temperature is lowered.

Introduction

Fine powders of semiconducting oxides with deposited metal and/or metal oxide particles have been widely used as heterogeneous photocatalysts for innumerable chemical reactions. Among the many photocatalytic reactions, splitting of water assisted by light has become one of the most active areas in the use of heterogeneous photocatalysis, since it can be a promising chemical route for energy renewal and energy storage. $BaTi_4O_9$ combined with RuO_2 is one of such photocatalysts for water decomposition that has recently emerged as a new class of materials.[1−4]

One of the serious problems in studying this new composite material as a photocatalyst is the great difficulty in preparing the host $BaTi_4O_9$ compound in its pure form at relatively low temperatures, viz. 700−900 °C. For instance, $BaTi_4O_9$ has been synthesized by the conventional ceramic route, which involves mixing $BaCO_3$ and TiO_2, followed by repeated cycles of grinding and firing at high temperatures (1000−1300 °C).[5−8] Alternatively, attempts to synthesize $BaTi_4O_9$ at lower temperatures have been carried out by sol−gel techniques using metal alkoxides, but unexpectedly, firing the gels at 1100[9] or 1300 °C[10] was required to obtain phase pure $BaTi_4O_9$. The large grain growth owing to the high-temperature heat treatment is therefore a principal obstacle to the application of $BaTi_4O_9$ as a host for the photocatalytic composite material with higher activities. To solve this problem, we previously developed a simple Pechini-type polymerizable complex (PC)

* To whom all correspondence should be addressed. E-mail: kakihana@rlem.titech.ac.jp.

(1) Inoue, Y.; Kubokawa, T.; Sato, K. *J. Chem. Soc., Chem. Commun.* **1990**, 1298.
(2) Inoue, Y.; Kubokawa, T.; Sato, K. *J. Phys. Chem.* **1991**, *95*, 4095.
(3) Inoue, Y.; Niiyama, T.; Asai, Y.; Sato, K. *J. Chem. Soc., Chem. Commun.* **1992**, 579.
(4) Inoue, Y.; Asai, Y.; Sato, K. *J. Chem. Soc., Faraday Trans.* **1994**, *90*, 797.
(5) Mhaisalkar, S. G.; Lee, W. E.; Readey, D. W. *J. Am. Ceram. Soc.* **1989**, *72*, 2154.
(6) O'Bryan, Jr. H. M.; Thomson, J., Jr.; Ploudre, J. K. *J. Am. Ceram. Soc.* **1974**, *57*, 450.
(7) Lukaszewicz, K. *Proc. Chem.* **1957**, *31*, 1111.
(8) Rase, D. E.; Roy, R. *J. Am. Ceram. Soc.* **1955**, *38*, 102.

10.1021/cm9804012 CCC: $18.00
Published on Web 12/15/1998

route,[11−15] based on polyesterification between citric acid (CA) and ethylene glycol (EG), that has been successfully used to synthesize pure $BaTi_4O_9$ at 700 °C.[16] The $BaTi_4O_9$ obtained via the PC route, combined with RuO_2, exhibited ∼2 times larger photocatalytic activities for the decomposition of water compared to that for a sample prepared by a traditional ceramic method at 1000 °C.[16] However, the $RuO_2/BaTi_4O_9$ material via the PC route showed photocatalytic activities much less than those expected from its relatively large surface area (∼20 m^2/g compared with 1−5 m^2/g for the sample via the high-temperature ceramic route). The reason for this irregularity remains unresolved.

This paper describes the details of the synthesis of $BaTi_4O_9$ by the PC route and the influence of preparation temperature (thereby the specific surface areas of products) on the photocatalytic activity for the decomposition of water in the $RuO_2/BaTi_4O_9$ material. To gain an insight into the origin of the less pronounced improvement in the photocatalytic activity mentioned above, the emission lifetimes were measured for three representative samples, synthesized at 700, 800, and 900 °C by the PC method, with surface areas of 20.4, 7.6, and 3.5 m^2/g, respectively. The results have shown an increase in the lifetime with a decrease in the surface area, suggesting a decrease in the number of defects in the crystals with an increase in the preparation temperature.

Experimental Section

(a) Preparation of the Host $BaTi_4O_9$. Powders of $BaTi_4O_9$ were synthesized by the PC method, as summarized in Figure 1. Described below is the process for preparing ∼4 g of $BaTi_4O_9$. Titanium tetraisopropoxide $\{Ti[OCH(CH_3)_2]_4 \equiv Ti(OiPr)_4\}$ and barium carbonate ($BaCO_3$) were chosen as the sources of titanium and barium, respectively. Ethylene glycol ($HOCH_2$-$CH_2OH \equiv$ EG) was used as a solvent in the initial stage of processing, while anhydrous citric acid ($HOOCCH_2C(OH)$-$(COOH)CH_2COOH \equiv$ CA) was used as a complexing agent to stabilize Ba and Ti ions against water evolved during the polyesterification between EG and CA at the later stage of processing. A 40 mmol portion of $Ti(OiPr)_4$ (11.4 g) was dissolved into 1.6 mol of EG (99.2 g ∼ 92 mL), followed by addition of CA (0.4 mol = 76.8 g) with continuous stirring to convert $Ti(OiPr)_4$ to stable Ti−CA complexes. After achieving complete dissolution of the CA, 10 mmol of $BaCO_3$ (1.97 g) was added and the mixture was magnetically stirred for 1 h at ∼50 °C to drive off the carbon dioxide evolved in the decomposition reaction of barium carbonate to produce a clear solution containing Ba− and Ti−CA complexes. The clear solution thus prepared, while stirred with a magnetic stirrer, was heated at ∼130 °C to promote esterification reactions between CA and EG and to remove the excess solvents. During the continued reaction at 130 °C, the solution became more viscous with vigorous evolution of foam accompanied by a change in color from colorless to deep yellow (or even brown), and finally it gelled without any visible precipitation or turbidity. Charring of the viscous polymeric gel at 350 °C for 2 h in a box furnace resulted in a black solid mass, which was lightly ground into a powder with a Teflon rod. The powder thus obtained is referred to as the "powder precursor" hereafter. The powder precursor was heat-treated in a furnace in static air at temperatures between 650 and 900 °C with an interval of 50 °C.

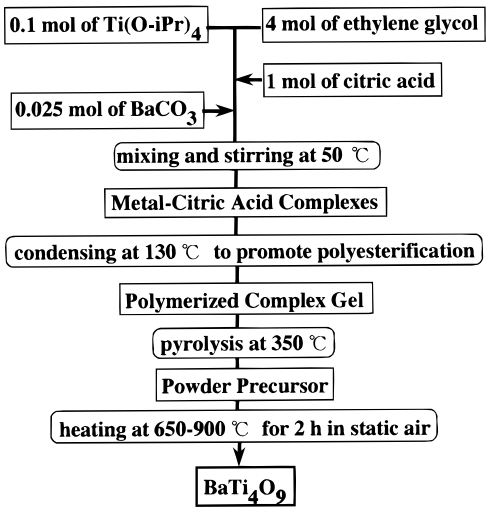

Figure 1. Flowchart for the polymerizable complex (PC) procedure used to prepare $BaTi_4O_9$.

For the purpose of comparison, $BaTi_4O_9$ was also prepared by the conventional ceramic route based on a solid-state reaction at 1100 °C for 10 h using an intimate mixture of $BaCO_3$ and TiO_2 achieved by mechanical grinding for 2 h.

(b) Preparation of Nanocomposite $RuO_2/BaTi_4O_9$. Photocatalytic composite materials are typically made by impregnation of a powder of the host compound with an aqueous solution of a metal salt, followed by appropriate heat treatments. Both powders of $BaTi_4O_9$ via the PC and the ceramic route were combined with a fixed amount of RuO_2 (1 wt % of Ru relative to $BaTi_4O_9$) in exactly the same manner as described below. Powders of $BaTi_4O_9$ were suspended into aqueous solutions containing $RuCl_3$, and the suspension was stirred for 4 h at ∼70 °C until most of the water was evaporated. An appropriate amount of water was again added, and the same procedure was repeated once more. The resulting mass was dried at 100 °C for 12 h. The impregnated $BaTi_4O_9$ was heat treated at 500 °C for 2 h under flowing H_2/N_2 gas (H_2 2% + N_2 98%) with a flow rate of 200 mL/min, followed by oxidation at 475 °C under flowing air with a flow rate of 200 mL/min for 7 h.

(c) Characterization. The products were characterized by X-ray diffraction (XRD) using Cu Kα radiation (MAC-Science, MXP^{3VA}) and Raman scattering with excitation using the 514.5 nm line of an Ar laser (Jobin-Yvon/Atago Bussan, T64000) to identify various possible phases formed. The specific surface area of the samples was measured by the conventional three-points BET method using nitrogen gas as absorbent (Coulter, SA3100). Ultraviolet−visible (UV−vis) diffuse reflectance spectra were measured for the products using a Shimadzu UV-2400PC spectrometer to evaluate their absorption edges (thereby band gap energies). The powdered $RuO_2/BaTi_4O_9$ photocatalysts (0.2 g of each) were suspended in 600 mL of pure water. The photodecomposition of water by $RuO_2/BaTi_4O_9$ was then carried out at 60 °C in a closed gas-circulation reaction vessel made of quartz glass under irradiation of light from a high-pressure Hg lamp operated at 100 W. H_2/O_2 gases evolved were analyzed every 30 min for a total reaction time of 5 h by gas chromatography. Observations and elemental analyses of RuO_2 nanoparticles on $BaTi_4O_9$ surfaces by trans-

(9) Phule, P. P.; Risbud, S. H. (*Better Ceramics through Chemistry III*; Brinker, C. J., Clark, D. E., Ulrich, D. R., Eds.) *Mater. Res. Soc. Symp. Proc.* **1988**, *121*, 275.
(10) Ritter, J. J.; Roth, R. S.; Blendell, J. E. *J. Am. Ceram. Soc.* **1986**, *69*, 155.
(11) Pechini, M. P. U.S. Patent 3,330,697, 1967.
(12) Kakihana, M. *J. Sol Gel Sci. Technol.* **1996**, *6*, 7.
(13) Eror, N. G.; Anderson, H. U. (In *Better Ceramics Through Chemistry II;* Brinker, C. J., Clark, D. E., Ulrich, D. R., Eds.) *Mater. Res. Soc. Proc.* **1986**, *73*, 571.
(14) Anderson, H. U.; Pennell, M. J.; Guha, J. P. In *Advances in Ceramics*: *Ceramic Powder Science;* Messing, G. L., Mazdiyasni, K. S., McCauley, J. W., Harber, R. A., Eds.; Am. Ceram. Soc.: Westerville, OH, 1987; Vol. 21, p 91.
(15) Lessing, P. A. *Am. Ceram. Soc. Bull.* **1989**, *168*, 1002.
(16) Kakihana, M.; Arima, M.; Sato, T.; Yoshida, K.; Yamashita, Y.; Yashima, M.; Yoshimura, M. *Appl. Phys. Lett.* **1996**, *69*, 2053.

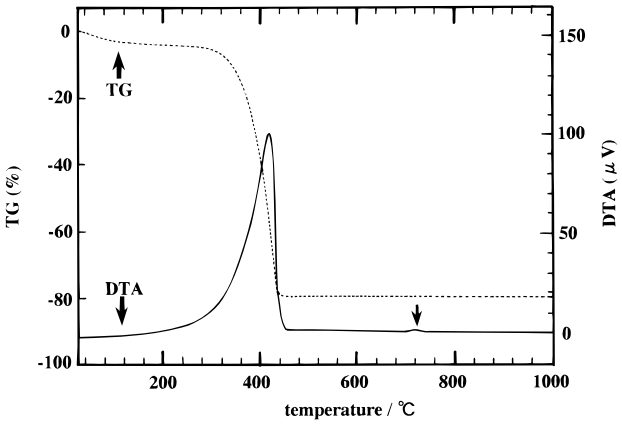

Figure 2. TG−DTA curves of the powder precursor in air with a heating rate 2 °C/min.

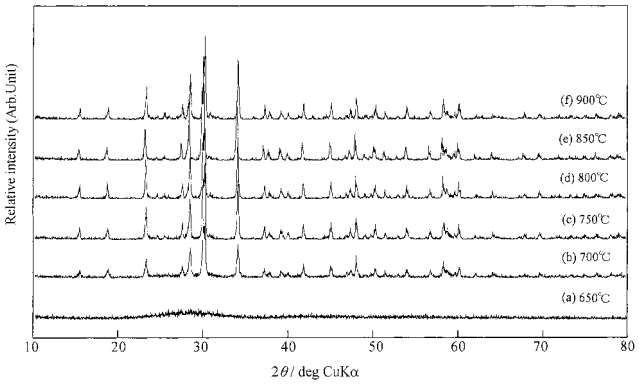

Figure 3. X-ray diffraction patterns of products obtained by heating the powder precursor in static air for 2 h at 650 °C (a), 700 °C (b), 750 °C (c), 800 °C (d), 850 °C (e), and 900 °C (f).

mission electron microscopy were performed with a JEOL JEM-2010 electron transmission microscope operated at 200 kV. The emission lifetimes were measured using an nitrodye laser (Hamamatsu Photonics LN120C) with a pulse width of 200 ps, an imaging monochromator/spectrograph (Acton Research Corp. Spectro Pro-1), a digital delay pulse generator (Stanford Research System DG535), a streak scope (Hamamatsu Photonics, C4334), and a data analyzing system (Power Macintosh 7100/80AV with an analyzing program of Hamamatsu Photonics Photolumi 2.44f ACT).

Results and Discussion

(a) Structural Evolution of $BaTi_4O_9$. Figure 2 illustrates the TG and DTA curves of the powder precursor fired in air using a heating rate of 2 °C/min in the temperature range of 25 and 1000 °C. The TG curve indicates a continuously small weight loss up to ∼300 °C, another large weight loss extending up to ∼440 °C, and no further weight loss up to 1000 °C. The first weight loss is mostly due to dehydration and evaporation of volatile organic components. The second large weight loss between 300 and 440 °C can be ascribed to decomposition of the organics contained in the powder precursor. Any clear plateaus, indicating formation of well-defined intermediate decomposition products, were not identified between 300 and 440 °C on the TG curve. In view of the fact that there is no further weight loss above 440 °C up to 1000 °C, it is inferred that the decomposition product at temperatures higher than 440 °C contains neither distinct carbonate-related intermediate phases (including isolated $BaCO_3$) nor isolated carbons. The DTA scan of the powder precursor at a heating rate of 2 °C/min in static air shows a large exothermic feature corresponding to the large weight loss observed by TG between 300 and 440 °C, which can be attributed to burnout of most of the organics contained in the powder precursor. A weak but significant exothermic feature starting at ∼700 °C (marked with an arrow) in the DTA curve can probably be attributed to the onset of crystallization into $BaTi_4O_9$, since this is not accompanied by a weight loss. Crystallization of $BaTi_4O_9$ at ∼700 °C has indeed been confirmed by XRD, as discussed below (Figure 3). The XRD patterns of powders obtained after calcining the powder precursor in air at six different temperatures for 2 h are shown in Figure 3 in the 2θ range of 10°−80°. The powder precursors heat treated above 650 °C were all white, which was usually indicative of complete burnout of the residual carbon, consistent with the TG−DTA analysis (Figure 2). The powder precursor fired at 650 °C was primarily amorphous in structure, with only a broad continuum being observed in the XRD (Figure 3a). Substantial crystallization occurred during the heat treatment of the powder precursor in air at 700 °C for 2 h (Figure 3b). The width of the principal lines somewhat sharpens when the calcination temperature is increased (Figure 3b → 3c−f), but the overall shape of the pattern remains almost unchanged. We were, however, aware of a very broad continuum in 2θ range of 25°−35° from a close inspection of the XRD pattern in Figure 3b, suggesting imperfect crystallization of the sample heat-treated at 700 °C. (This residual amorphous component appears to affect the photocatalytic activity of $RuO_2/BaTi_4O_9$ in a negative way, as shown later.) All the well-defined peaks in the XRD patterns of Figure 3b−f exhibited a pure orthorhombic phase of $BaTi_4O_9$, in good agreement with the diffraction pattern observed for this compound by Phule et al.[9] It should be stressed here that the impurity phases $BaTi_5O_{11}$, $Ba_4Ti_{13}O_{30}$, and $BaTi_2O_5$, which are most frequently formed as byproducts during the synthesis of $BaTi_4O_9$,[9,10] were not detected by XRD.

The purity of the $BaTi_4O_9$ sample was also checked by Raman spectroscopy, a technique which is capable of detecting impurities consisting of very small crystallites not easily identified with the XRD technique because of their diffuse reflections. A representative Raman pattern of a powder obtained after calcining the powder precursor in air at 700 °C for 2 h is shown in Figure 4 in a frequency range of 60−1200 cm^{-1}, where all the lines coincide well in both position and relative intensities with those of the orthorhombic $BaTi_4O_9$.[17] The Raman spectrum also shows no evidence for the presence of $BaCO_3$ because of the complete absence of the strongest Raman peak at 1059 cm^{-1} characteristic of $BaCO_3$.

(b) UV−Vis Diffuse Reflectance Spectra of $BaTi_4O_9$. The UV−vis diffuse reflectance spectra of $BaTi_4O_9$ prepared at 700−900 °C are shown in Figure 5. The overall shape of each spectrum is basically the same with each other, but note that the band gap energy derived from the absorption edge for the sample prepared at 700 °C (3.57 eV) appears to be slightly smaller

(17) Javadpour, J.; Eror, N. G. *J. Am. Ceram. Soc.* **1988**, *71*, 206.

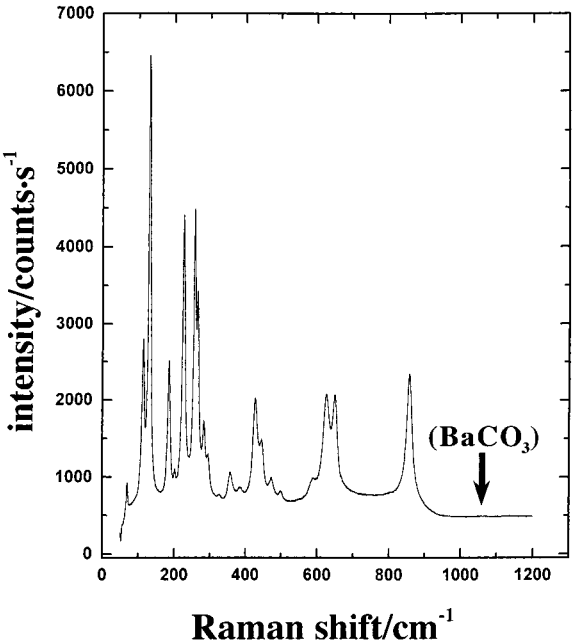

Figure 4. A Raman spectrum of a product obtained by heating the powder precursor in static air for 2 h at 700 °C.

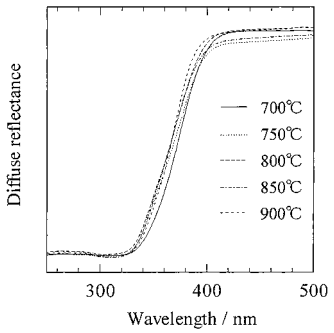

Figure 5. UV−vis diffuse reflectance spectra of PC-$BaTi_4O_9$ samples prepared at 700−900 °C.

than those (3.67 eV in average) for the other samples heat-treated at 750−900 °C. This would in turn indicate that the overall electronic state of $BaTi_4O_9$ prepared at 700 °C differs slightly from those for the other four $BaTi_4O_9$ samples synthesized at higher temperatures, and it could probably be related to the imperfect crystallization of $BaTi_4O_9$ at 700 °C as revealed by the XRD measurement (Figure 3a).

(c) Photocatalytic Activities of $RuO_2/BaTi_4O_9$. Figure 6 shows the H_2 gas evolution volumes with illumination time for $RuO_2/BaTi_4O_9$ samples prepared at 700−900 °C by the PC route, and their photocatalytic activity is compared with that of another sample prepared at 1100 °C by the conventional ceramic route. The corresponding O_2 gas evolution volumes were confirmed to be from nearly equal to half the volume of H_2 gas for all the samples tested (see Figure 7); i.e., H_2O is stoichiometrically decomposed into H_2 and $^1/_2O_2$. The rate of the H_2 and O_2 gas evolution for the RuO_2/PC-$BaTi_4O_9$ samples is plotted as a function of the preparation temperature in Figure 7, wherein data for the specific surface area of each sample is also included. As expected from the low surface area (<1 m^2/g) of the $RuO_2/BaTi_4O_9$ prepared by the conventional ceramic route at 1100 °C, its photocatalytic activity (~130 $\mu mol \cdot h^{-1} \cdot g^{-1}$ for H_2 evolution) was the lowest among the

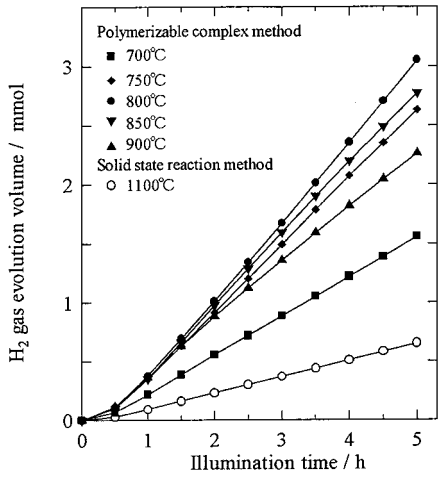

Figure 6. H_2 gas evolution volumes with illumination time for various $RuO_2/BaTi_4O_9$ samples. The host $BaTi_4O_9$ powders were prepared by the PC method at 700 °C (■), 750 °C (◆), 800 °C (●), 850 °C (▼), and 900 °C (▲) or by the conventional ceramic route at 1100 °C (○). The amount of RuO_2 is the same for all the $BaTi_4O_9$ powders (1 wt % of Ru relative to $BaTi_4O_9$). The weight of each catalyst used for test is 0.2 g, and the volume is expressed in units per gram of catalyst.

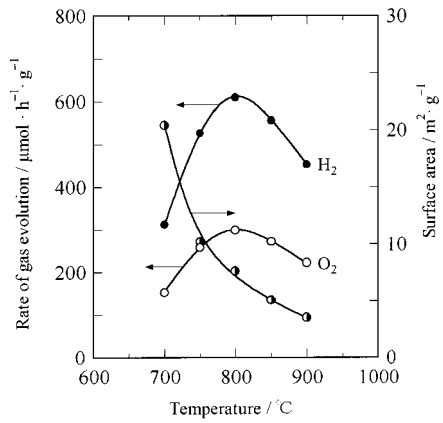

Figure 7. The rate of gas evolution (●, H_2; ○, O_2) and the specific surface area (◑) for the RuO_2/PC-$BaTi_4O_9$ samples as a function of preparation temperature.

others (see Figure 6). Quite interestingly, however, the RuO_2/PC-$BaTi_4O_9$ sample prepared at 700 °C showed a photocatalytic activity of only ~310 $\mu mol \cdot h^{-1} \cdot g^{-1}$ for H_2 evolution, which is much less than that expected from its relatively large surface area (20.4 m^2/g). On the contrary, the photocatalytic activity for H_2 evolution is increased with a decrease in the surface area from 20.4 down to 7.6 m^2/g, and it reached a maximum value of ~610 $\mu mol \cdot h^{-1} \cdot g^{-1}$ for the sample prepared at 800 °C, despite its lower surface area (7.6 m^2/g). One possible explanation for this contradiction can be offered, if one takes into consideration that the host $BaTi_4O_9$ compound prepared at 700 °C contains imperfections or defects in the lattice, which arise from the imperfect crystallization at low temperatures (as indeed revealed by XRD; see Figure 3 and the text). These defects may act as recombination centers for photoinduced electrons and holes, thus reducing the net photocatalytic activity significantly. The idea that the surface reactivities of the poorly crystallized samples were suppressed by defects acting as election-hole traps was recently proposed by Ohtani et al.[18] for an amorphous−anatase mixture of TiO_2 particles and by Stone at al.[19] for TiO_2

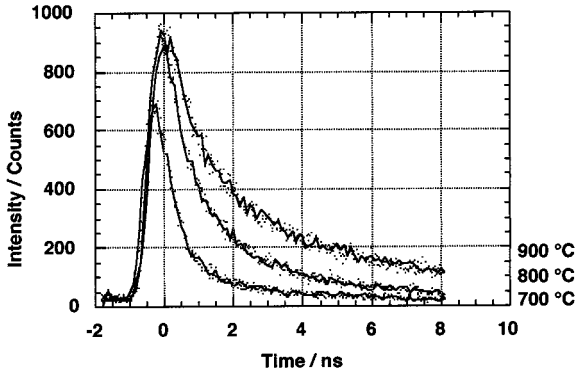

Figure 8. Emission decay curves for the RuO_2/PC-$BaTi_4O_9$ samples prepared at 700, 800, and 900 °C. The wavelength of the laser used for excitation is 337.1 nm.

Table 1. The Emission Lifetimes τ_1 and τ_2 and the Average Emission Lifetime $\langle\tau\rangle$ for Representative Samples Prepared at 700, 800, and 900 °C

temp,[a] °C	parameter[b]		lifetime/ns		
	A_1	A_2	τ_1	τ_2	$\langle\tau\rangle$[c]
900	0.011	0.026	5.12 ± 0.05	0.744 ± 0.006	4.0
800	0.010	0.033	3.90 ± 0.03	0.534 ± 0.004	2.9
700	0.008	0.039	3.83 ± 0.03	0.530 ± 0.004	2.5

[a] Temperatures at which the host $BaTi_4O_9$ has been prepared. [b] $I = A_1 \exp(-t/\tau_1) + A_2 \exp(-t/\tau_2)$. [c] $\langle\tau\rangle = \sum_{i=0}^{i=n} A_i\tau_i^2/\sum_{i=0}^{i=n} A_i\tau_i$.

and Nb_2O_5 mesoporous molecular sieves. To gain further insight into this anomalous effect, emission spectra and their decay curves were measured for three representative samples prepared at 700, 800, and 900 °C, each with a respective surface area of 20.4, 7.6, and 3.4 m^2/g, the results of which are shown in Figure 8. The emission decay curve (Figure 8) was then analyzed using the double-exponential law shown in eq 1[20]

$$I(t) = A_1 \exp(-t/\tau_1) + A_2 \exp(-t/\tau_2) \qquad (1)$$

where $I(t)$, A, and τ denote the emission intensity at time t, a pre-exponential parameter, and the emission lifetime, respectively, and they were evaluated (see Table 1). Average emission lifetimes $\langle\tau\rangle$ defined as eq 2[20,21] (shown in the last column in Table 1) can then be calculated using these fitted parameters:

$$\langle\tau\rangle = [A_1{\tau_1}^2 + A_2{\tau_2}^2]/[A_1\tau_1 + A_2\tau_2] \qquad (2)$$

The immediate conclusion drawn from Figure 8 and Table 1 is that the average emission lifetime is increased from 2.5 ns up to 4.0 ns with an increase in the preparation temperature. This result would suggest that the number of lattice defects acting as inactivation centers is decreased as the preparation temperature is increased. A similar and more extensive argument has been advanced by Uchida et al.[20] for photocatalytic composite materials in the forms of $H_2Ti_4O_9$/(TiO_2, Pt) and $H_4Nb_6O_{17}$/(TiO_2, Pt).

The unexpected larger photocatalytic activity in RuO_2/PC-$BaTi_4O_9$ prepared at 800 °C can now be explained by taking into account the balance of two conflicting factors that affect the overall photocatalytic activity. When the processing temperature for $BaTi_4O_9$ is increased from 700 to 800 °C, the expected increment of the photocatalytic activity owing to the decrease in the number of lattice defects may exceed the expected decrement of the photocatalytic activity owing to the decrease in the surface area. For genuine crystals of $BaTi_4O_9$ practically free from any defects, the photocatalytic activity should then be primarily governed by their surface area. This was indeed confirmed by the observation of the strong reduction in the photocatalytic activity with an increase in the preparation temperature from 800 to 900 °C (see Figures 6 and 7); i.e., the decrement of the photocatalytic activity is almost consistent with what is expected from a decrease in the surface area (Figure 7). Thus the remarkable acceleration of the photocatalytic reaction in the RuO_2/PC-$BaTi_4O_9$ sample prepared at 800 °C can be considered as a consequence of utilizing such a well-optimized sample with respect to the balance between the crystallinity and the surface area.

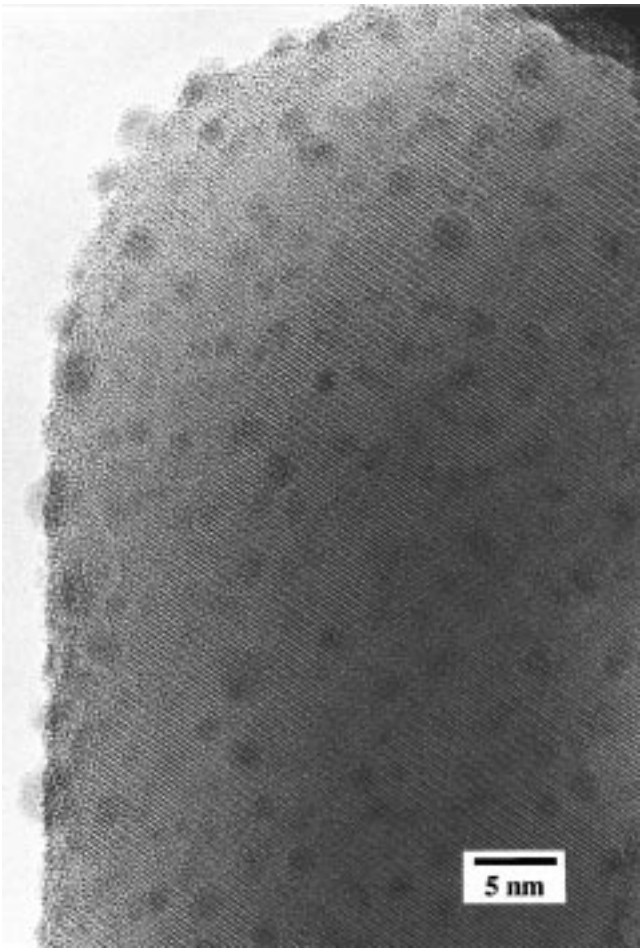

Figure 9. A high-resolution transmission electron microscopic image of RuO_2/PC-$BaTi_4O_9$ (1 wt % Ru relative to $BaTi_4O_9$) prepared at 800 °C. The dark spots correspond to RuO_2 particles.

(d) High-Resolution Electron Microscopic Image of $RuO_2/BaTi_4O_9$. The $BaTi_4O_9$ compound is characterized by the presence of the pentagonal-prism tunnel structure, which has been supposed to prevent aggregation of RuO_2 particles.[2−4] Figure 9 shows a high-resolution electron microscopic image for the RuO_2/PC-

(18) Ohtani, B.; Ogawa, Y.; Nishimoti, S. *J. Phys. Chem.* **1997**, *101*, 3746.
(19) Stone, Jr., V. F.; Davis, R. J. *Chem. Mater.* **1998**, *10*, 1468.
(20) Uchida, S.; Yamamoto, Y.; Fujishiro, Y.; Watanabe, A.; Ito, O.; Sato, T. *J. Chem. Soc., Faraday Trans.* **1997**, *93*, 3229.
(21) James, D. R.; Liu, Y. S.; Mayo, P. De; Ware, W. R. *Chem. Phys. Lett.* **1985**, *120*, 460.

$BaTi_4O_9$ sample prepared at 800 °C. A number of dark spots ~2 nm in diameter are homogeneously distributed on the surface of $BaTi_4O_9$, and from the energy analysis of the characteristic X-ray peak they were confirmed to be composed of RuO_2. Since the photocatalytic process can be influenced not only by the particle size and the crystallinity of the host $BaTi_4O_9$ but also by how evenly and how finely the RuO_2 is distributed over the surface of $BaTi_4O_9$, the observed uniform dispersion of ultrafine spherical RuO_2 particles shown in Figure 9 would be another reason for the highest activity of the RuO_2/PC-$BaTi_4O_9$ material prepared at 800 °C. It should be noted that when the amount of RuO_2 is fixed, the dispersion and particle size of RuO_2 may depend on the surface area, thus affecting the photocatalytic activity. To clarify this issue, a thorough TEM characterization on RuO_2/$BaTi_4O_9$ materials as functions of the surface area and the amount of RuO_2 will be required as a future subject.

Conclusion

Pure $BaTi_4O_9$ has been successfully synthesized by heat-treating the PC powder precursors in air at reduced temperatures (700−900 °C) for 2 h. The success in lowering the processing temperature for $BaTi_4O_9$ implies that the molecular-level mixing of Ba and Ti seems to be likely throughout the PC process. The PC route is a promising methodology for preparing $BaTi_4O_9$ with relatively large surface areas that can be subsequently used as a highly active nanocomposite RuO_2/$BaTi_4O_9$ photocatalyst for water decomposition. It has been shown that the overall photocatalytic activity is governed not only by the specific surface area but also by the number of lattice defects. Emission lifetime measurements have suggested that samples prepared at lower temperatures tend to contain an increased number of defects in the lattice, which may act as recombination centers for photoinduced electrons and holes, thus reducing the net photocatalytic activity significantly.

Acknowledgment. Financial support by "Research for the Future" Program no. JSPS-RFTF96R06901 from The Japan Society for the Promotion of Science is greatly acknowledged. The assistance of Mr. K. Ibe (Electron Optics Division, JEOL Ltd.) with TEM observations is greatly appreciated.

CM9804012